Contents lists available at Science-Gate

International Journal of Advanced and Applied Sciences

Journal homepage: http://www.science-gate.com/IJAAS.html

Mineralogy of the unified soil classes of Wadi As Suqah: A sustainable engineering geology approach

Musaad A. Alotabi, Mohammed A. M. Alghamdi *

Engineering Geology Department, Faculty of Earth Sciences, King Abdulaziz University, Jeddah, Saudi Arabia

ARTICLE INFO

Article history:
Received 2 July 2022
Received in revised form
16 May 2023
Accepted 28 May 2023

Keywords:
Soil classification
Minerals
Mining
Construction
Sustainability goals

ABSTRACT

This research endeavors to enhance soil classification methodologies in alignment with sustainability goals for mining and construction activities. The study focuses on the evaluation, classification, and mapping of quaternary surface deposits in Wadi As Suqah. To achieve this objective, an integration of mineral analyses and unified soil classes was employed. Various research methods were utilized, including Geographic Information Systems (GIS), sieve analysis, Atterberg limits, and X-ray diffraction. Additionally, principal component analysis (PCA) on variance was employed to identify the most influential minerals within the deposits. Consequently, a sophisticated engineering geological map of the deposited category was created, resulting in the categorization of Wadi As Suqah into 13 groups (A, B, C, …, L) based on similar lithofacies. These groups further represented 7 clusters of mineral-based classes, such as quartz-anorthite or quartz-albite, leading to the formation of 5 unified soil classes, namely SP, SP-SM, SM, SC-SM, and SC. Among the classified groups, group C, characterized by rich sandy quartz with some albite content, emerged as the largest group, occupying 20.3% of the total area. Conversely, group M, consisting of rich fine anorthite with a trace of quartz, constituted the minor group, representing only 0.5% of the entire area. The study acknowledges the limitations of being confined to surface investigations and, therefore, strongly recommends further subsurface investigations for a more comprehensive geotechnical understanding. The findings of this research hold significant implications for sustainable mining and construction practices by enabling a refined soil classification approach based on mineral composition and unified soil classes.

1. Introduction

Iwuji et al. (2016) stated that sustainable development deals with the exploitation of the earth's resources without depletion (extraction exceeds the rate of renewal) or consumption of the resources of future generations. The sustainability aspect of geomaterials for construction is connected to the optimum employment of geotechnical properties in specific applications (Přikryl et al., 2016). Paige-Green (2011) assured that engineering geology investigation should be adapted to maximize resource sustainability for Long Linear constructions.

In addition, characterizing geological materials to provide fundamental societal needs is one of the key roles covered by the United Nations Sustainable Development Goals (SDGs) (Lagesse et al., 2022). The soil fraction mineralogy is required for sustainable management (Ajiboye et al., 2019). A variety of methods may help categorize soils, such as geology, mineralogy, particle size, and plasticity index, in the proper context (Coduto et al., 2010). The unified soil classification system (USCS) (ASTM, 2010) is based on grain size, liquid limit, and plasticity index (Das and Sobhan, 2013).

Mineralogy and chemical composition significantly affect bulk sediment grain size distributions (Zhou et al., 2015). The geochemical composition of sediment affected particle size (Weltje and von Eynatten, 2004). Folk (1954) Proposed that identifying sedimentary rocks can be best by grain size, textural maturity, and mineral composition. Bartholomay et al. (1989) and Von Eynatten and Tolosana Delgado (2011) suggested that mineralogy data are consistent with grain-size

* Corresponding Author.
Email Address: mmushrif@kau.edu.sa (M. A. M. Alghamdi)
https://doi.org/10.21833/ijaas.2023.07.016
Corresponding author's ORCID profile:
https://orcid.org/0000-0002-7790-5698

data. Neopane and Sujakhu (2013) found that mineral and grain size content varies as the sediment flows from headwork to tailrace downstream.

Alghamdi and Hegazy (2013) and Alghamdi (2018) proposed a significant positive and strong correlation between dolomite and fine grain size of silty sand soil in Wadi Arar sediment. Previous research studies have merged more than a variable of characteristics, such as minerals and grain size, for the geotechnical evaluation of sediments.

On the other hand, due to integrating mineralogy and soil class, Akpokodje (1985) asserted that the engineering classification of some Australian arid zone soils is based mainly on the quantitative presence of minerals. Varnes and Keaton (1984) explained that engineering geological information could be effectively represented in a map with basic data on resource evaluation, which are essential in organized planning.

In light of the increasing population growth, it needs to rationalize consumption and sustain the sediments for mining and construction. Therefore, as an early stage of sustainability management, it is necessary to assess and classify the deposit of Wadi As Suqah using a modern engineering geology approach.

2. Aim and purpose

Accordingly, this study answers the following two questions: First, regarding soil classes, minerals, and merging between them, what is the classification and distribution of the surficial soil resources of Wadi As Suqah? Second, by which method can this happen? Consequently, geological engineering maps of the soil classes and minerals distribution are produced to facilitate the selection of appropriate materials for specific mining or construction. Furthermore, the information provided is intended to help homeowners, contractors, and municipalities have more options of resources available to select what will achieve long-term sustainability.

3. Geological setting

As presented in Fig. 1, the 422 km² study region is a part of the Western Arabian Shield, including igneous and plutonic rock complexes. The central area consists of Usfan and Shumaysi formations overlaid by basaltic lava flows (El-Didy, 1998). Usfan formation consists of sandstone, shale, marls, and wedges of fossiliferous carbonate, while Shumaysi formation is composed of sandstone, siltstone, and Oolitic ironstone bands (El-Didy, 1998).

On the other hand, Quaternary surface sediments (sand and gravel) are spread along broad valleys until coastal regions (Spencer and Vincent, 1984). Kotb et al. (1988) mentioned that the Wadi's upstream area has alternating stones in layers with coarse sand, while the downstream has silt and clayey silt alterations.

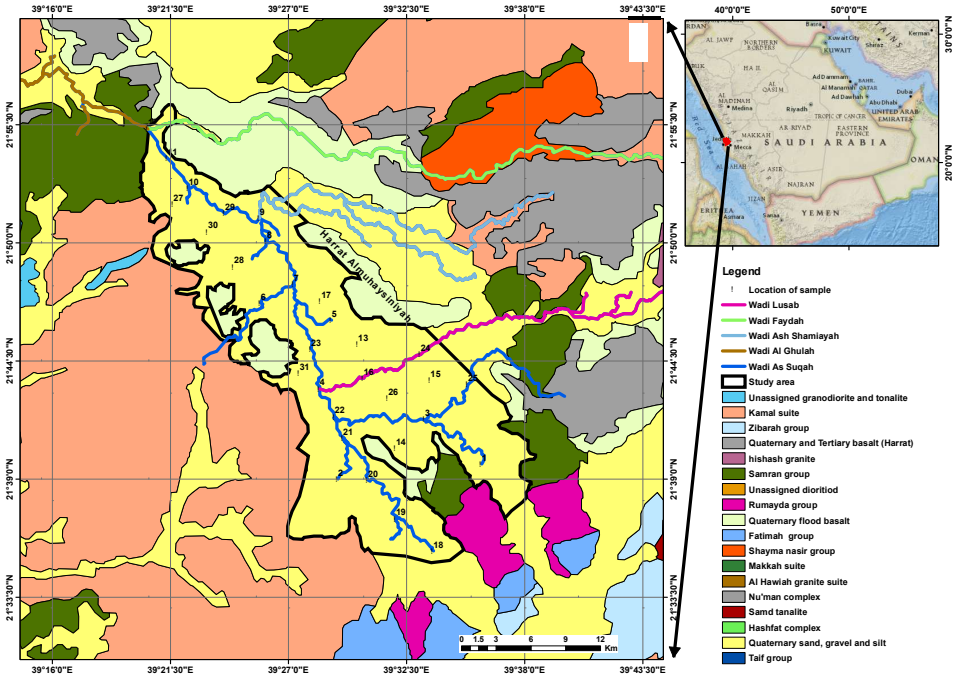

Fig. 1: Digital geological map modified after Moore and Al-Rehaili (1989) included sampling locations

4. Methodology

From the sample collection to the geological engineering maps, Fig. 2 illustrates three stages of the workflow of this article. Firstly, based on the grain size content and Atterberg limits, soil classes were deduced to produce the geological engineering map of soil class distribution. Secondly, X-ray

diffraction (XRD) and Principle component analysis (PCA) were employed to identify the most effective minerals (Vidal et al., 2016). Then, 3D clustering was used for categorizing and mapping the effective minerals. Third stage concerns merging soil class with minerals to produce a sophisticated engineering geological map. This advanced approach was applied for the first time compared to previous studies.

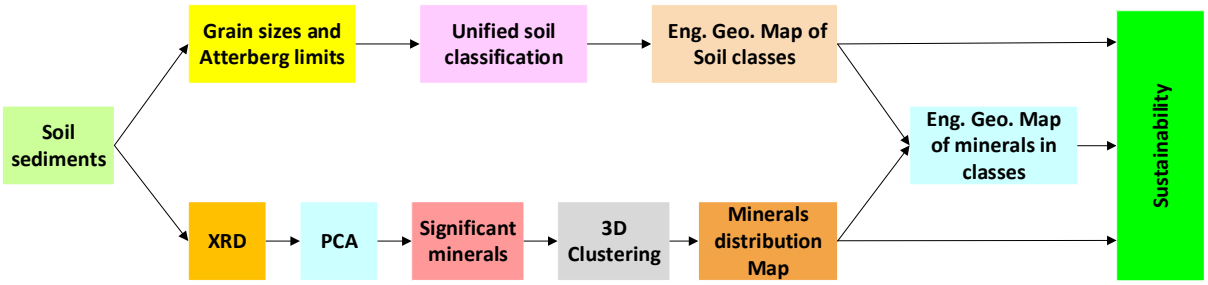

Fig. 2: Graphical abstract of methodology

4.1. Sampling

Based on Wadi As Suqah's geology, geomorphology, and drainage pattern, thirty-one surficial samples are collected from the confluence of the tributaries Fig. 1. One kg of each sample is collected by shovel and then saved in a sealed plastic bag. Finally, the samples were stored at room temperature to be ready for laboratory testing.

4.2. Soil classification

The laboratory tests were conducted at the Saudi Geological Survey, while the soil samples were classified according to the unified soil classification system (ASTM, 2010).

4.3. Mineralogical analysis

3D modeling, mosaicing, and matching with previous literature, such as Alwash et al. (1986) and Spencer et al. (1988), were used for mineralogy analysis and mapping, as shown in the following chart Fig. 3.

The mineral compositions are identified using the X-ray diffraction (XRD) method facilities at the Egyptian Petroleum Ministry. PAN analytical XRD Diffraction equipment model is used with specifications including X'Pert PRO with Secondary Monochromator, Cu-radiation (λ=1.542Å) at 45 kV, 35 MA, and scanning speed 0.04°/sec. Diffraction peaks vary between 2θ=20° and 60 °, corresponding to spacing (d, Å) and relative intensities (1/1).

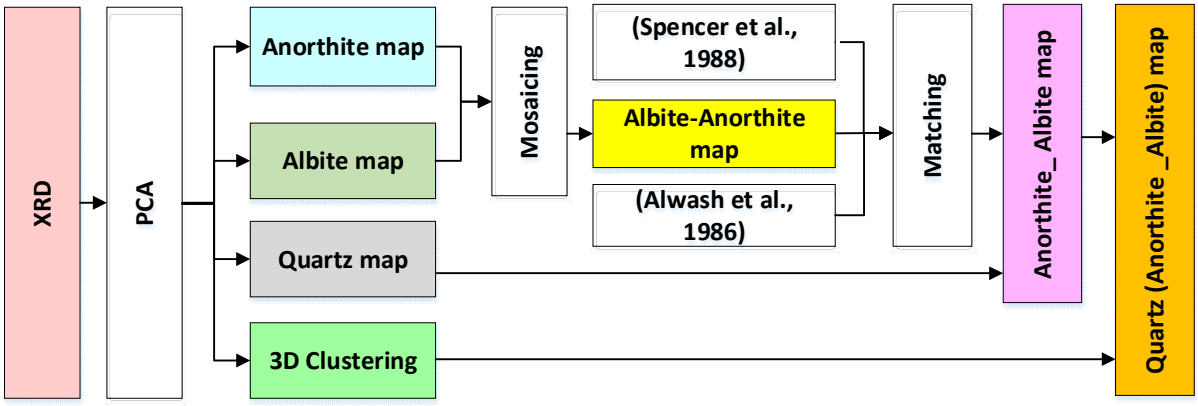

Fig. 3: Mineralogy mapping approach

4.4. Statistical analysis

PCA was used to evaluate the geochemical elements at different grain sizes (Chandrajith et al., 2001). Also, Makvandi et al. (2019) used this method as an advanced tool for provenance discrimination and indicator mineral exploration. PCA for covariance is used to find the main variables that are effective in the reaction of phenomenon behavior. Moreover, 3D cluster analysis is also used to classify Wadi sediment from mineralogical viewpoints. Finally, MS Excel v16 and its Adds application, such as XLSTAT, are employed for comprehensive statistical analysis.

4.5. Geographic information system (GIS)

A robust mapping and analytics software, Arc GIS version (10.4.1), has been used for mapping purposes. The Inverse Distance Weighted (IDW) tool in Arc GIS was used to produce engineering geological maps of soil classes and minerals.

5. Result and analysis

In addition to the grain size content (gravel, sand, and fine fractions) investigated by Alotaibi and Alghamdi (2022), Table 1 presents the Atterberg limits, including the plastic limit (PL), liquid limit (LL), and plasticity index (PI), which were utilized to discern the unified soil classes along Wadi As Suqah. Furthermore, Table 2 provides details on the mineralogy content of Wadi As Suqah and its corresponding locations. To streamline the dataset and identify the primary influential variables, the PCA (Principal Component Analysis) processing involved the utilization of the covariance matrix, as shown in Table 3. This approach allowed for the reduction of the twelve variables (comprising nine minerals and three grain size fractions). Additionally, a biplot (Fig. 4) was employed to visually represent the results of the PCA, depicting relationships among minerals, soil classes, and grain size. The PCA Biplot analysis revealed that approximately 69.65% of the data variability could be explained. PC1 (F1 axis) accounted for 45.22% of the total variance in the data, while PC2 (F2 axis) represented 24.43%.

Table 1: Unified soil classifications based on grain size content and the Atterberg limit

Count	Sample No.	Latitude E	Longitude N	Gravel%	Sand%	Fine%	PL%	LL%	PI%	USCS
1	S1	21 39 42	39 36 00	3.5	92.2	4.3	NP	NV	NP	SP
2	S2	21 39 0.002	39 29 18.001	1.2	90.5	8.1	NP	NV	NP	SP-SM
3	S3	21 41 45	39 33 21	0.3	97.4	2.3	NP	NV	NP	SP
4	S4	21 43 12	39 28 27	0.5	98	1.2	NP	NV	NP	SP
5	S5	21 46 24.002	39 29 0.001	18.2	63	18.8	23	27	4	SM.
6	S6	21 47 12	39 25 42	0	97.5	2.5	NP	NV	NP	SP
7	S7	21 48 3	39 27 15	14.8	84.1	1.1	NP	NV	NP	SP
8	S8	21 50 3.002	39 26 0.001	1.5	76.2	22.3	NP	NV	NP	SM
9	S9	21 51 9.002	39 25 39.001	0	60.9	39.1	16	22	6	SC-SM
10	S10	21 52 31	39 22 22	0.2	83.7	16.1	NP	NV	NP	SM
11	S11	21 53 55.67	39 21 22.33	0	59	41	14	18	4	SC-SM
12	S12	21 55 18.002	39 20 27.001	7.6	91.6	0.8	NP	NV	NP	SP
13	S13	21 45 1	39 30 16	1.5	85	13.5	NP	NV	NP	SM
14	S14	21 40 25.89	39 31 59.71	1.3	92.1	6.6	NP	NV	NP	SP-SM
15	S15	21 43 36.40	39 33 36.98	1	67	32	NP	NV	NP	SM
16	S16	21 43 42	39 30 30	2.2	79.8	18	NP	NV	NP	SM
17	S17	21 47 16.45	39 28 31.1	17.9	67.7	12.5	15	25	10	SC
18	S18	21 35 39	39 33 45	1.9	97.2	0.9	NP	NV	NP	SP
19	S19	21 37 9.0	39 32 00	1.8	94.5	3.7	NP	NV	NP	SP
20	S20	21 38 57	39 30 42.001	2.4	97.4	0.2	NP	NV	NP	SP
21	S21	21 40 54	39 29 33	0	90	10	NP	NV	NP	SP-SM
22	S22	21 41 54	39 29 09	9.1	89.3	1.6	NP	NV	NP	SP
23	S23	21 44 59	39 28 17	0	78.1	21.9	NP	NV	NP	SM
24	S24	21 44 48.002	39 33 9.001	0.5	91.8	7.7	NP	NV	NP	SP-SM
25	S25	21 43 24	39 38 21	3.9	88.4	7.7	NP	NV	NP	SP-SM
26	S26	21 42 44.921	39 31 38.703	1.9	88.8	9.3	NP	NV	NP	SP-SM
27	S27	21 51 47.46	39 21 38.38	0.3	95.7	4	NP	NV	NP	SP
28	S28	21 48 52.717	39 24 27.996	0.57	87.9	11.5	NP	NV	NP	SP-SM
29	S29	21 51 21.002	39 24 3.001	0	86.78	13.21	NP	NV	NP	SM
30	S30	21 50 30.79	39 23 15.57	3.5	80	16.5	NP	NV	NP	SM
31	S31	21 43 54	39 27 31	0	86.7	13.3	NP	NV	NP	SM

SP: Poorly graded sands, gravelly sands, little or no fines; SP-SM: Poorly graded sand with silt; SM: Silty sands, sand-silt mixtures; SC-SM: Clayey-silty sand, sand-silt-clay mixtures; SC: Clayey sands, sand-clay mixtures according to ASTM (2010)

Table 2: The minerals contents among Wadi As Suqah

Count	Sample No.	Latitude E	Longitude N	Quartz %	Anorthite %	Albite %	Actinolite %	Mont. %	Kao. %	Diopside %	Calcite %	Halite %
1	S1	21 39 42	39 36 00	80	0	15	5	0	0	0	0	0
2	S2	21 39 0.002	39 29 18.001	75	22	0	3	0	0	0	0	0
3	S3	21 41 45	39 33 21	80	19	0	0	0	1	0	0	0
4	S4	21 43 12	39 28 27	59	0	36	5	0	0	0	0	0
5	S5	21 46 24.002	39 29 0.001	60	20	0	10	5	5	0	0	0
6	S6	21 47 12	39 25 42	75	0	23	2	0	0	0	0	0
7	S7	21 48 3	39 27 15	63	32	0	5	0	0	0	0	0
8	S8	21 50 3.002	39 26 0.001	52	0	35	13	0	0	0	0	0
9	S9	21 51 9.002	39 25 39.001	60	0	25	0	15	0	0	0	0
10	S10	21 52 31	39 22 22	58	0	42	0	0	0	0	0	0
11	S11	21 53 55.67	39 21 22.33	40	0	30	20	10	0	0	0	0
12	S12	21 55 18.002	39 20 27.001	77	0	20	0	0	3	0	0	0
13	S13	21 45 1	39 30 16	67	25	0	5	3	0	0	0	0
14	S14	21 40 25.89	39 31 59.71	80	10	0	5	0	0	0	5	0
15	S15	21 43 36.40	39 33 36.98	50	0	40	0	5	5	0	0	0
16	S16	21 43 42	39 30 30	65	0	15	13	7	0	0	0	0
17	S17	21 47 16.45	39 28 31.1	55	37	0	0	0	8	0	0	0
18	S18	21 35 39	39 33 45	45	0	35	15	0	5	0	0	0
19	S19	21 37 9.0	39 32 00	80	15	0	5	0	0	0	0	0
20	S20	21 38 57	39 30 42.001	55	0	45	0	0	0	0	0	0
21	S21	21 40 54	39 29 33	55	40	0	5	0	0	0	0	0
22	S22	21 41 54	39 29 09	56	44	0	0	0	0	0	0	0
23	S23	21 44 59	39 28 17	56	36	0	8	0	0	0	0	0
24	S24	21 44 48.002	39 33 9.001	55	30	0	10	5	0	0	0	0
25	S25	21 43 24	39 38 21	60	40	0	0	0	0	0	0	0
26	S26	21 42 44.921	39 31 38.703	30	25	0	0	5	0	40	0	0
27	S27	21 51 47.46	39 21 38.38	58	40	0	0	0	0	0	0	2
28	S28	21 48 52.717	39 24 27.996	60	40	0	0	0	0	0	0	0
29	S29	21 51 21.002	39 24 3.001	55	25	0	20	0	0	0	0	0
30	S30	21 50 30.79	39 23 15.57	75	20	0	0	2	3	0	0	0
31	S31	21 43 54	39 27 31	63	0	0	37	0	0	0	0	0
		Average		61	17	12	6	1.83	0.96	1	0.16	0.05

Table 3: Covariance matrix

	Gravel %	Sand %	Fine %	Quartz %	Anorthite %	Albite %	Actinolite %	Mont. %	Kao.%	Diopside %	Calcite %	Halite %
Gravel %	**24.98746**	-17.896	-7.953	1.015	22.469	-19.526	-6.491	-1.436	6.061	-1.610	-0.298	-0.184
Sand %	-17.896	**123.7404**	-104.940	45.551	15.177	-19.381	-12.948	-26.482	-8.496	4.767	1.128	0.683
Fine %	-7.953	-104.940	**112.9664**	-46.245	-38.782	39.475	19.837	28.062	2.021	-3.056	-0.817	-0.495
Quartz %	1.015	45.551	-46.245	**143.9334**	-22.039	-49.812	-18.516	-13.249	-2.798	-40.333	3.023	-0.210
Anorthite %	22.469	15.177	-38.782	-22.039	**259.5942**	-195.338	-37.290	-15.036	-0.911	10.614	-1.093	1.498
Albite %	-19.526	-19.381	39.475	-49.812	-195.338	**252.7451**	-2.903	10.201	2.763	-15.026	-1.878	-0.751
Actinolite %	-6.491	-12.948	19.837	-18.516	-37.290	-2.903	**66.70968**	2.065	-1.774	-7.742	-0.161	-0.387
Mont. %	-1.436	-26.482	28.062	-13.249	-15.036	10.201	2.065	**12.32882**	0.027	4.079	-0.297	-0.119
kao. %	6.061	-8.496	2.021	-2.798	-0.911	2.763	-1.774	0.027	**4.16025**	-1.249	-0.156	-0.062
Diopside %	-1.610	4.767	-3.056	-40.333	10.614	-15.026	-7.742	4.079	-1.249	**49.94797**	-0.208	-0.083
Calcite %	-0.298	1.128	-0.817	3.023	-1.093	-1.878	-0.161	-0.297	-0.156	-0.208	**0.780437**	-0.010
Halite %	-0.184	0.683	-0.495	-0.210	1.498	-0.751	-0.387	-0.119	-0.062	-0.083	-0.010	**0.12487**

Values in bold are different from 0 with a significance level alpha +0.05

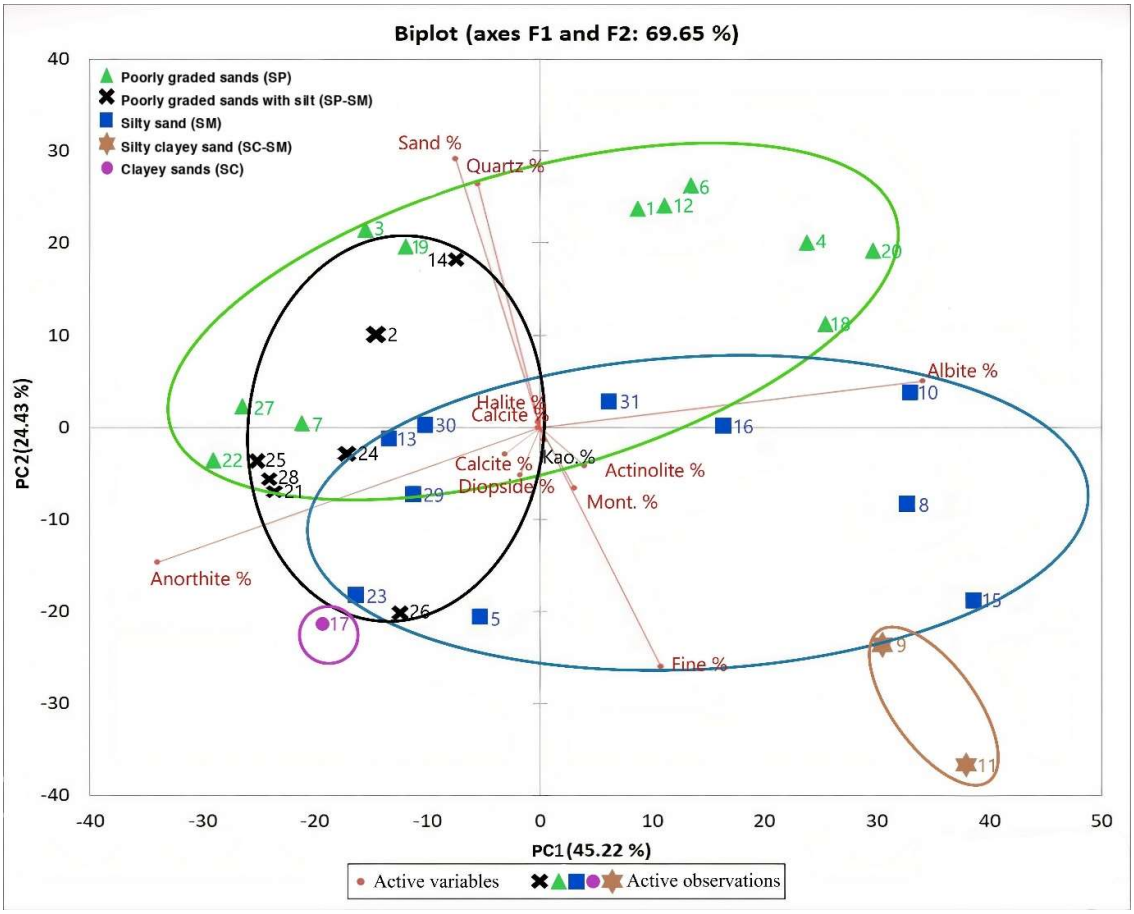

Fig. 4: Biplot of variables and observations

5.1. Distribution of the soil classes

The zoning process of the soil classes was executed on the basis of USCS and GIS, as illustrated in the work plan Fig. 5. Generally, from upstream to downstream, there is a gradual change in the distribution of soil classes over Wadi As Suqah, as shown in Fig. 6. It is noted that with 50.6%, poorly graded sands, gravelly sands, and little or no fines (SP) are present in upstream. On the other hand, the lithofacies change to silty sand as sand-silt mixtures (SM) with 31.9%. Finally, clayey sands and sand-clay mixtures (SC) occur at 0.5%. A mix of the previous type, SP-SM, occurs between SP and SM at 14.8% and SC- SM between SM and SC at 2.2%, as shown in Fig. 6. These changes may reflect the effect of geomorphology, structure, and deposit cycling.

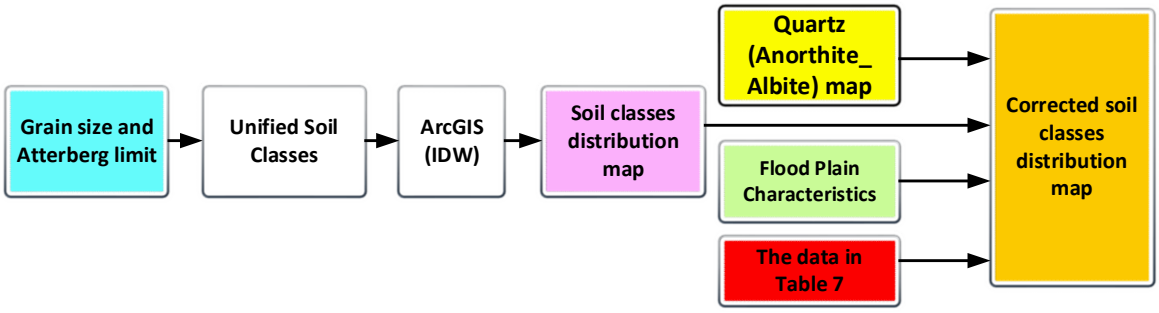

Fig. 5: Workflow of soil classes mapping

In the biplot, ellipses were drawn around each soil class to discriminate them Fig. 4. The stations of the SP class can be distinguished by (the green ellipse). In comparison to the PC2 spread, SP has an increasing spread from negative to positive of PC1, while it is only positive with PC2. Consequently, stations in the SM class (blue ellipse) are similar to SP propagation scores with PC1, but it has a negative spreading score with PC2. On the other hand, the stations of SP-SM class (the black ellipse) overlap with the SP and SM classes, but it is extended negatively with PC1 and spread along PC2. Otherwise, SC-SM (brown ellipse) are seated in the most positive of PC1 and highest negative of PC2. Finally, the SC class (pink ellipse), found at station 17, is located at an equal distance of negative scores of PC1 and PC2 on the biplot.

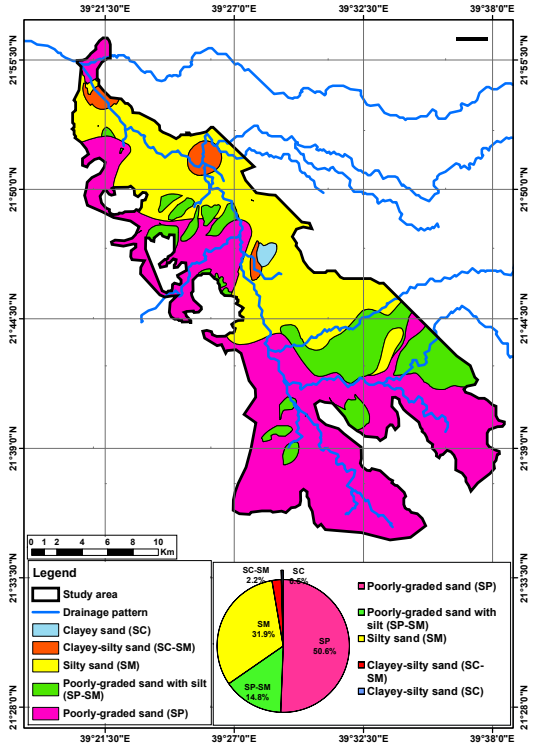

Fig. 6: Distribution of the soil classes of the surficial sediments

5.2. Mineralogy

As shown in Fig. 7, the average percentages for quartz, anorthite, albite, actinolite, montmorillonite, diopside, kaolinite, calcite, and halite are 61, 17, 12, 6, 1.83, 1, 0.96, 0.16, and 0.05, respectively. The maximum percentage content is 80, 44, 45, 37, 15, 40, 8, 5, and 2%, consecutively, while the minimum is zero % for the whole minerals except quartz was 30% Table 2. According to the biplot of PCA Fig. 4, the active variables (Red lines) represent the most effective minerals (quartz, anorthite, and albite) for both sizes, sand and fine. Based on the length of the representative lines and the angles between them, Quartz contents are correlated positively with sand size due to their lines pointing in similar directions. On the other hand, albite and anorthite don't correlate with grain sizes. However, there was a negative correlation between these two variables because their vectors were in opposite directions. The general characteristics of each effective mineral found in the study area are listed in Table 4. As shown in the minerals distribution maps in Figs. 8 and 9, anorthite and albite are not found in the same locations. Otherwise, four high concentrations spots of anorthite were observed. The first is located in the southeastern of the study area, while the second is in the southwestern. The third is adjacent to Harrat al-Muhaysiniyah, while the fourth surrounds the confluence area of Wadi Ash Shamiayah with Wadi As Suqah. Consequently, as shown in Fig. 10, quartz is present in the whole Wadi with varying proportions. Four locations in the study area reflect a high percentage of quartz: Upstream of the Wadi As Suqah, in the vicinity of Harrat Almuhaysiniyah, the opposite area of the confluence of Wadi Ash Shamiayah with Wadi As Suqah, and finally, at the downstream where the confluence of Wadi As Suqah with Wadi Faydah. For the clustering purpose of the essential minerals, a 3D model of their content and distribution was presented in Fig. 11. For more details and based on the similarity of the mineral content at different stations, the sediments of Wadi As Suqah were classified into six subclusters named A, B, C, D, E, and F. Subcluster A has moderate anorthite and low quartz concentration. In contrast, B has high anorthite and moderate quartz. Low anorthite and high quartz concentrations characterize subcluster C. Subcluster F has a reasonable content of quartz, while D has high quartz and moderate albite. Finally, subcluster E contains moderate quartz and high albite. As shown in Fig. 11 and according to the relative variation of their values, the study area can be categorized into

two main clusters, quartz-anorthite, and quartz-albite. According to comparing of anorthite and albite distribution, Fig. 12, with Alwash et al. (1986) and Spencer et al. (1988), it is found that the result matches both. Based on the previous, the environmental deposits' area of Wadi As Suqah may be classified as a flood plain and meandering filled with alluvial deposits, where anorthite is present in the alluvium of the flood plain, while albite is in the movable alluvium. The segregation occurred between them because anorthite is less stable than albite and has a higher specific gravity.

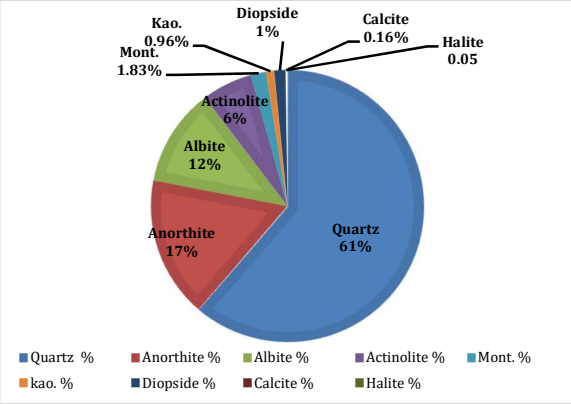

Fig. 7: Mineralogy content

5.3. Mineralogy of soil classes

Fig. 13 was produced to show an engineering geological map of the mineralogy of soil classes by combining the soil class distribution map, Fig. 6, with the mineral distribution map, Fig. 12.

As a result, seven zones, namely, poorly-graded sand of quartz-albite, silty sand of quartz-anorthite, poorly-graded sand of quartz-anorthite, poorly-graded sand with the silt of quartz-anorthite, silty sand of quartz-albite, silty clayey sand of quartz-albite and clayey sand of quartz-anorthite are shown on the engineering geological map. The area ratios for each zone are 35.6, 15, 14.7, 19.9, 12, 2.2, and 0.5%, respectively, Fig. 13. Table 5 summarizes the area of mineralogy in each soil class.

As shown in Fig. 4, mineralogy is presented in the whole soil class. Albite presented in SP, SM, and SC-SM at many locations. At the same time, additional SP-SM and SC classes anorthite appear in the same classes at the remaining study area sites except for SC-SM. Otherwise, from the point of view of PC2, quartz is the main mineral that influences SP and SP-SM.

6. Discussion and interpretation

To produce a specific soil classification that matches the sustainability goals, the mineral in soil class and groups of similar locations were shown on the biplot Fig. 14. Consequently, the study area has been categorized into 13 groups (A, B, C, ..., L) of similar lithofacies representing 7 clusters of mineral-based (quartz-anorthite or quartz-albite) to form 5 unified soil classes (SP, SP-SM, SM, SC-SM, and SC) Figs. 15 and 16.

The SP soil class is segmented into quartz-anorthite and quartz-albite clusters. Quartz-anorthite comprises A and B groups. Group A was more discriminatory with more anorthite than group B, while sandy quartz is more common in group B than A. Consequently, groups of the quartz-albite cluster (C and D) show that albite is more abundant in group D. Additionally, sandy quartz is more common in group C than in group D. Otherwise, SP-SM class which contains E, F, and G groups, has only a quartz-anorthite, whereas group F has more anorthite than E and G groups. Furthermore, quartz-anorthite and quartz-albite clusters make up the SM class. The quartz-anorthite cluster contains H and I groups and is characterized by a moderate to low fine anorthite. Otherwise, the cluster of quartz albite group has a strong effect for fine albite in group K compared to group J. Consequently, it was observed that SP has quartz-anorthite and quartz-albite more slightly than SM. Finally, each SC-SM and SC class contains one cluster and one group. They are characterized by a fine grain of albite and anorthite, respectively. It was observed that SP-SM and SC have no albite, while SC-SM has no anorthite. Alternatively, it may be observed that the M, E, and H groups represent different classes but have the same mineralogical and grain size effect, Fig. 14.

Table 4: General properties of the main minerals in Wadi As Suqah (Pellants, 1992)

	Anorthite	Albite	Quartz
Group	Silicates	Silicates	Silicates
Composition	CaAl2Si2O6	NaAlSi3O8	Sio2
Hardness	6-6.5	6-6.5	7
Specific gravity	2.74-2.76	2.6-2.63	2.65
Cleavage	Perfect	Distinct	None
Fracture	Conchoidal to uneven	Uneven	Conchoidal to uneven
Crystal system	Triclinic	Triclinic	Trigonal/ hexagonal

Table 5: Area of mineralogy in soil classes

	Sediment category	Area, km^2	Area, %
1	Poorly-graded sand of quartz-albite	150.48	35.6
2	Silty sand of quartz-anorthite	83.95	19.9
3	Poorly-graded sand of quartz-anorthite	63.28	15
4	Poorly-graded sand with silt of quartz-anorthite	62.43	14.7
5	Silty sand of quartz-albite	50.48	12
6	Silty-clayey sand of quartz-albite	9.6	2.2
7	Clayey sand of quartz-anorthite	1.99	0.5

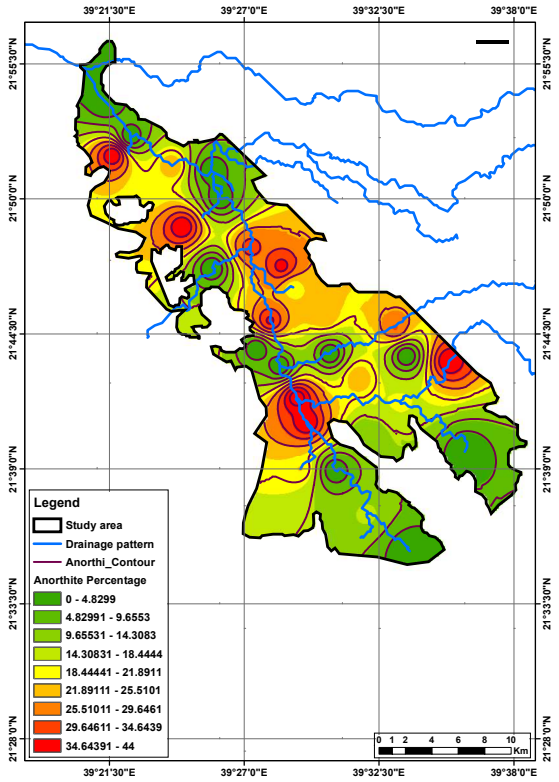

Fig. 8: Distribution of anorthite among Wadi As Suqah

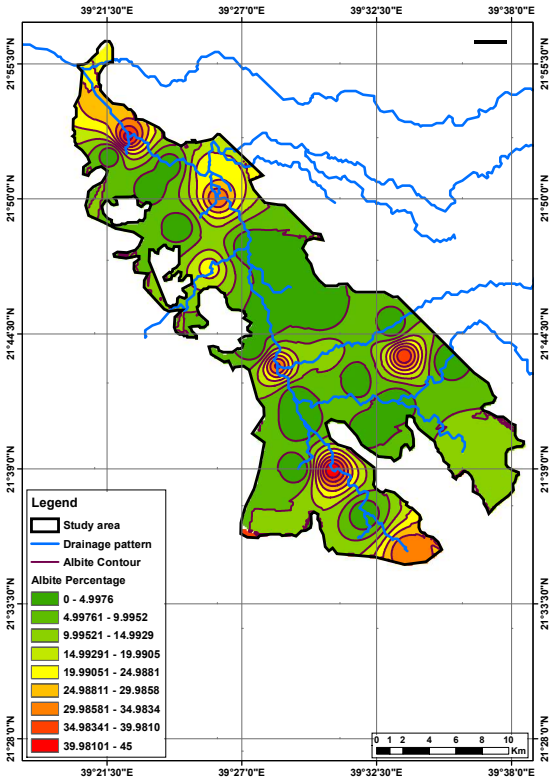

Fig. 9: Distribution of albite among Wadi As Suqah

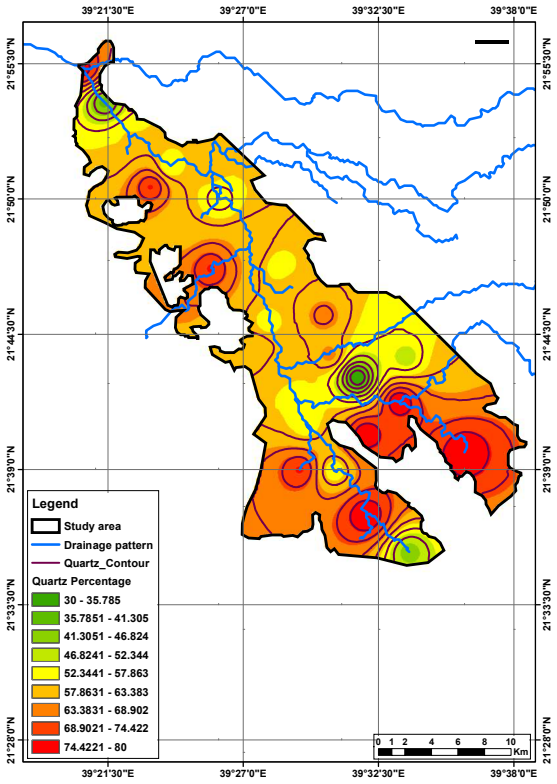

Fig. 10: Distribution of quartz among Wadi As Suqah

On the other hand, Group C represents the most extensive area with a percentage of 20.3%, followed by group D with 15.4% and group K with 11.7%. Otherwise, groups B, J, F, I, A, E, and H have an area percentage of 8.1, 8.1, 8, 7, 6.8, 5.2, and 5.1%, respectively. Furthermore, L, G, and M show the minor area percentage, with 2.2%, 1.6%, and 0.5%, respectively, as shown in Table 6. In terms of engineering geology, quartz concentration decreases with the transition from upstream to downstream, as

shown in Fig. 10. It occupies the maximum percentage in SP soils compared to other soil classes, with a ratio of 66, while the minimum in SC and SC-SM with 55% and 50%, respectively Table 7. On the other hand, quartz maintains its presence in all soil classes at least 20% higher than other minerals. SP has anorthite and albite at 2% above SM. Albite disappears in SP-SM and SC, while anorthite, with a content of 37% in SC, is higher than SP-SM by 7%. SC-SM behaves opposite to SP-SM, which has no anorthite and 27% of albite. SP, SC-SM, and SC have quartz, albite, and anorthite above the standard deviation. Otherwise, SC-SM values of quartz and anorthite contents are less than the standard deviation.

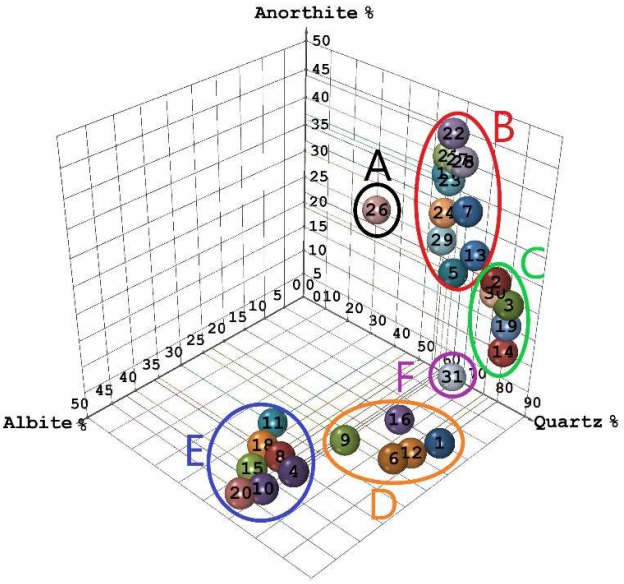

Fig. 11: 3D clustering of minerals of Wadi As Suqah

Table 6: Area of mineralogy groups in soil classes

	Sediment category	Area, km²	Area, %
A	SP of rich anorthite with some sandy quartz	28.76	6.8%
B	SP of rich sandy quartz with a trace of anorthite	34.33	8.1%
C	SP of rich sandy quartz with some albite	85.53	20.3%
D	SP of rich albite with some sandy quartz	64.95	15.4%
E	SP-SM of rich fine anorthite with a trace of quartz	22.11	5.2%
F	SP-SM of rich anorthite with a trace of sandy quartz	33.72	8%
G	SP-SM of rich sandy quartz with some anorthite	6.6	1.6%
H	SM of rich fine anorthite with a trace of quartz	21.36	5.1%
I	SM of some anorthite with a trace of sandy quartz	29.59	7%
J	SM of some albite with a trace of sandy quartz	34.18	8.1%
K	SM of fine rich albite with a trace of quartz	49.29	11.7%
L	SC-SM of rich fine albite with a trace of quartz	1.9	0.5%
M	SC of rich fine anorthite with a trace of quartz	9.6	2.2%

Table 7: The average content and standard deviation (SD) of mineralogy for different soil classes

Soil class	Count of station	Average of quartz %	Average of anorthite %	Average of albite %
SP	11	66.2	13.6	15.8
SP-SM	7	59.3	29.6	0
SM	10	60.1	12.6	13.2
SC-SM	2	50	0	27.5
SC	1	55	37	0
Mean		58.1	18.6	11.3
SD		6	14.7	11.6

Red (more than SD), magenta (less than SD), and grey (has no albite)

Considering the integration between the mineral distribution and the engineering soil classes of Wadi As Suqah to clarify the optimal use of these resources to achieve its sustainability, numerous products rely on quartz for various purposes, including filters and absorbents, foundry sand, fillers, and abrasives. In addition, optical fibers and other high-tech products are made from a special class of ultra-pure quartz (Vatalis et al., 2015), while anorthite and albite are used to manufacture glass and ceramics. The SP class is reasonably stable in embankment applications, while the SM and SC classes are fairly stable. In terms of compacting, the SP and SM classes are good, while the SC is fair in compacting. Otherwise, the SP, SM, and SC classes have a good to poor bearing value in foundation usages depending on the density (USAEWES, 1953). So that mineralogy can support the USCS to increase soil functionality in mining and construction.

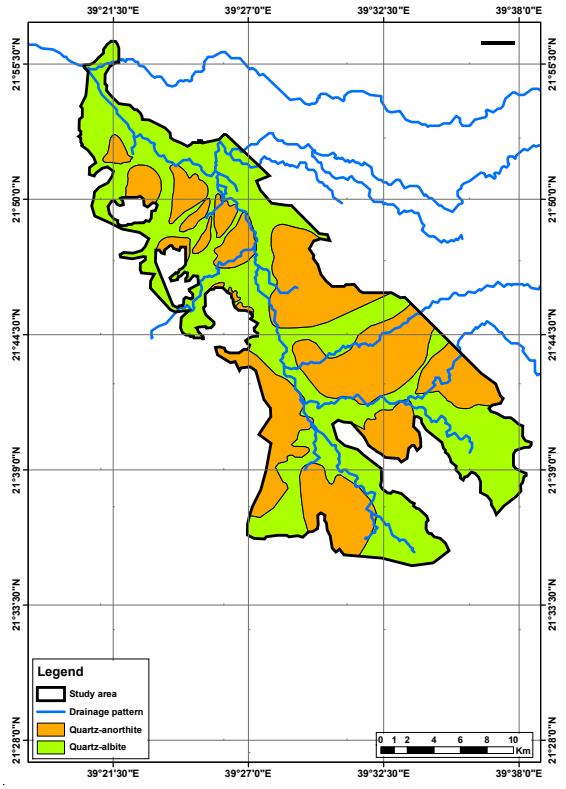

Fig. 12: Distribution of quartz-anorthite and quartz-albite

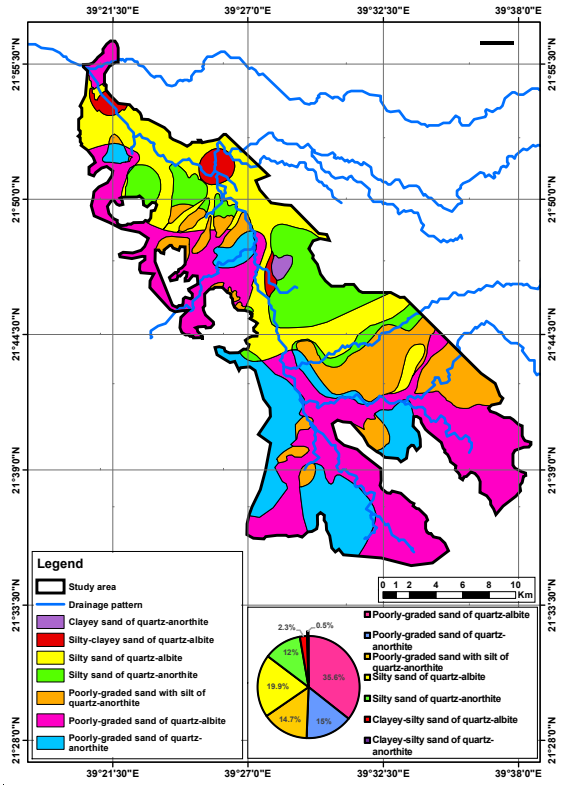

Fig. 13: Engineering geology map of mineralogy and unified soil classes

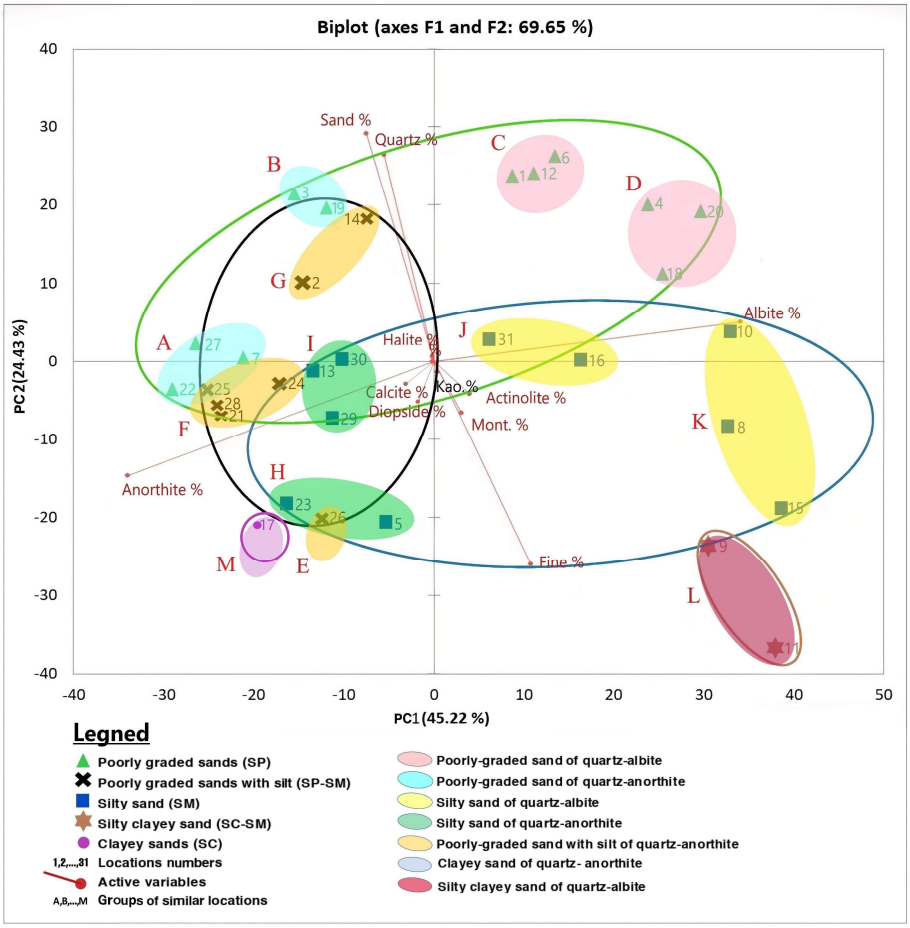

Fig. 14: Biplot of variables (loading) and observations (scores)

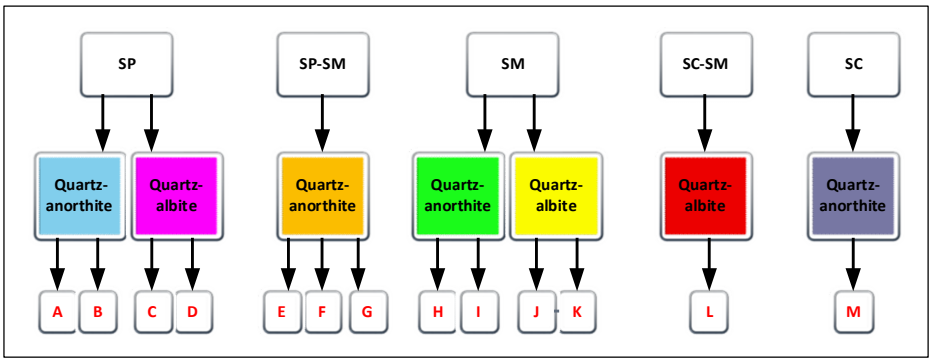

Fig. 15: Grouping of mineralogy within the soil classes

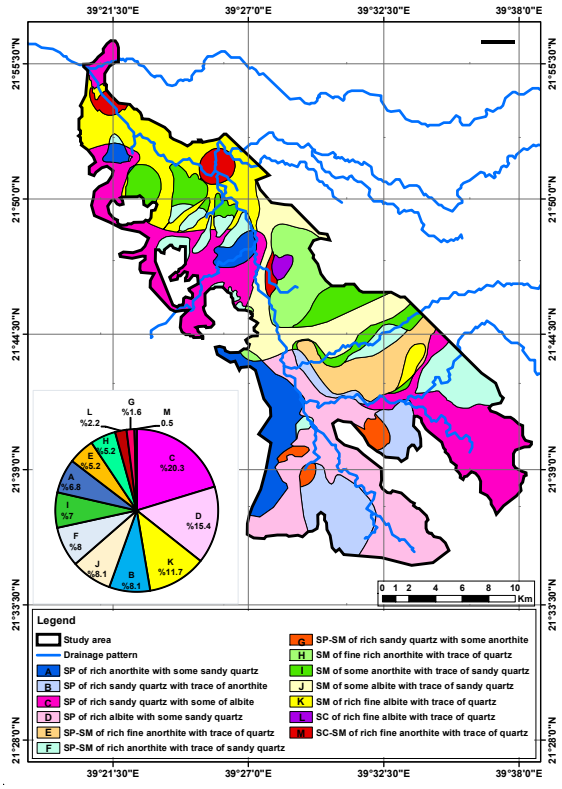

Fig. 16: Engineering geology map of mineralogy groups in soil classes

7. Conclusions and recommendations

Based on the geostatistical engineering approach, the geomaterial of Wadi As Suqah can be sustained in the light of the following significant findings:

1. The study area has been categorized into 13 groups (A, B, C, …, L) of similar lithofacies representing 7 clusters of mineral-based (quartz-anorthite or quartz-albite) to form 5 unified soil classes (SP, SP-SM, SM, SC-SM, and SC).
2. SP class occupied 50.6% of the total 422 km^2 of the study area, while SM, SP-SM, SC-SM, and SC represent 31.9%, 14.8%, 2.2%, and 0.5%, respectively
3. SP has quartz, anorthite, and albite slightly more than SM.
4. According to each class's mineral contents, poorly graded sand of quartz-albite covers the largest area, representing 35.6%. On the other hand, the smallest zone is clayey-silty sand of quartz-anorthite, which covers nearly 0.5%.
5. Group C (SP of rich sandy quartz with some albite) represents the largest area of Wadi As Suqah with 20.3%, while Group M (SC of rich fine anorthite with a trace of quartz) is the smallest with 0.5%.
6. SP-SM and SC have no albite, while SC-SM has no anorthite.
7. Merging mineralogical classification with the unified soil classification system increases the functionality of soils in mining and construction.
8. Since this article is a surface concentration study, a subsurface investigation is recommended to determine deposition thickness and geotechnical properties.

Compliance with ethical standards

Conflict of interest

The author(s) declared no potential conflicts of interest with respect to the research, authorship, and/or publication of this article.

References

Ajiboye GA, Oyetunji CA, Mesele SA, and Talbot J (2019). The role of soil mineralogical characteristics in sustainable soil fertility management: A case study of some tropical Alfisols in Nigeria. Communications in Soil Science and Plant Analysis, 50(3): 333-349. https://doi.org/10.1080/00103624.2018.1563100

Akpokodje EG (1985). The engineering classification of some Australian arid zone soils. Bulletin of the International Association of Engineering Geology, 31(1): 5-8. https://doi.org/10.1007/BF02594741

Alghamdi MA (2018). Relationship between grain size distribution and radon content in surficial sediments of Wadi Arar, Saudi Arabia. Engineering, Technology and Applied Science Research, 8(1): 2447-2451. https://doi.org/10.48084/etasr.1698

Alghamdi MA and Hegazy AA (2013). Physical properties of soil sediment in Wadi Arar, Kingdom of Saudi Arabia. International Journal of Civil Engineering, 2(5): 1-8.

Alotaibi MA and Alghamdi MAM (2022). Evaluation of grain size distribution of Wadi as Suqah, Northeast of Jeddah, Saudi Arabia. International Journal of Advanced and Applied Sciences, 9(9): 61–69. https://doi.org/10.21833/ijaas.2022.09.008

Alwash MA, Zaidi SMS, and Terhalle U (1986). Description of arid geomorphic features using Landsat-TM data and ground truth

information (Wadi Fatima, Kingdom of Saudi Arabia). CATENA, 13(3): 277-293. https://doi.org/10.1016/0341-8162(86)90003-2

ASTM (2010). ASTM D2487-17: Standard practice for classification of soils for engineering purposes (Unified Soil Classification System). ASTM International, West Conshohocken, USA.

Bartholomay RC, Knobel LL, and Davis LC (1989). Mineralogy and grain size of surficial sediment from the Big Lost River drainage and vicinity, with chemical and physical characteristics of geologic materials from selected sites at the Idaho National Engineering Laboratory, Idaho. Open-File Report 89-384, US Geological Survey, U.S. Department of Energy, Idaho Falls, USA. https://doi.org/10.3133/ofr89384

Chandrajith R, Dissanayake CB, and Tobschall HJ (2001). Application of multi-element relationships in stream sediments to mineral exploration: A case study of Walawe Ganga Basin, Sri Lanka. Applied Geochemistry, 16(3): 339-350. https://doi.org/10.1016/S0883-2927(00)00038-X

Coduto DP, Yeung MC, and Kitch WA (2010). Geotechnical engineering: Principles and practices. 2nd Edition, Pearson, London, UK.

Das BM and Sobhan K (2013). Principles of Geotechnical Engineering. 8th Edition, Cengage Learning, Stamford, USA.

El-Didy SM (1998). Hydrologic calculations in Wadis Hada Al Sham and Usfan. Meteorology, Environment and Arid Land Agriculture Sciences, 9(1): 159–177. https://doi.org/10.4197/met.9-1.13

Folk RL (1954). The distinction between grain size and mineral composition in sedimentary-rock nomenclature. The Journal of Geology, 62(4): 344-359. https://doi.org/10.1086/626171

Iwuji CC, Okeke OC, Ezenwoke BC, Amadi CC, and Nwachukwu H (2016). Earth resources exploitation and sustainable development: Geological and engineering perspectives. Engineering, 8(1): 21-33. https://doi.org/10.4236/eng.2016.81003

Kotb H, Zaidi SM, and Hakim H (1988). Hydrochemical characteristics of groundwater in the Usfan Basin, Saudi Arabia. Earth Sciences, 1(1): 113-132. https://doi.org/10.4197/Ear.1-1.6

Lagesse RH, Hambling J, Gill JC, Dobbs M, Lim C, and Ingvorsen P (2022). The role of engineering geology in delivering the United Nations sustainable development goals. Quarterly Journal of Engineering Geology and Hydrogeology, 55(3): qjegh2021-127. https://doi.org/10.1144/qjegh2021-127

Makvandi S, Beaudoin G, McClenaghan MB, Quirt D, and Ledru P (2019). PCA of Fe-oxides MLA data as an advanced tool in provenance discrimination and indicator mineral exploration: Case study from bedrock and till from the Kiggavik U deposits area (Nunavut, Canada). Journal of Geochemical Exploration, 197: 199-211. https://doi.org/10.1016/j.gexplo.2018.11.013

Moore TA and Al-Rehaili MH (1989). Geologic map of the Makkah quadrangle, sheet 21D, Kingdom of Saudi Arabia. Ministry of Petroleum and Mineral Resources, Jeddah, Saudi Arabia.

Neopane HP and Sujakhu S (2013). Particle size distribution and mineral analysis of sediments in Nepalese hydropower plant: A case study of Jhimruk hydropower plant. Kathmandu University Journal of Science, Engineering and Technology, 9(1): 29-36.

Paige-Green P (2011). Sustainability issues related to the engineering geology of long linear developments. Journal of Mountain Science, 8: 321-327. https://doi.org/10.1007/s11629-011-2110-y

Pellants C (1992). Rocks and minerals. Dorling Kindersley Publishers, London, UK.

Přikryl R, Török Á, Theodoridou M, Gomez-Heras M, and Miskovsky K (2016). Geomaterials in construction and their sustainability: Understanding their role in modern society. In: Přikryl R, Török Á, Gomez-Heras M, Miskovsky K, and Theodoridou M (Eds.), Sustainable use of traditional geomaterials in construction practice: 1-22. Volume 416, Geological Society, London, UK. https://doi.org/10.1144/SP416.21

Spencer CH and Vincent PL (1984). Bentonite resource potential and geology of the Cenozoic sediments. Open-File Report BRGM-OF-02-34, Saudi Arabian Deputy Ministry for Mineral Resources, Jeddah, Saudi Arabia.

Spencer CH, Cartier A, and Vincent PL (1988). Industrial mineral resources map of Jiddah, Kingdom of Saudi Arabia. Ministry of Petroleum and Mineral Resources, Jeddah, Saudi Arabia.

USAEWES (1953). The unified soil classification system: Technical memorandum No. 3–357. US Army Corps of Engineers, Waterways Experiment Station, Vicksburg, USA.

Varnes DJ and Keaton JR (1984). Trends in engineering geologic and related mapping 1972–1983. Bulletin of the Association of Engineering Geologists, 21(3): 255-267. https://doi.org/10.2113/gseegeosci.xxi.3.255

Vatalis KI, Charalambides G, and Benetis NP (2015). Market of high purity quartz innovative applications. Procedia Economics and Finance, 24: 734-742. https://doi.org/10.1016/S2212-5671(15)00688-7

Vidal R, Ma Y, Sastry SS, Vidal R, Ma Y, and Sastry SS (2016). Principal component analysis. In: Vidal R, Ma Y, and Sastry SS (Eds.), Generalized principal component analysis: 25-62. Volume 40, Springer New York, USA. https://doi.org/10.1007/978-0-387-87811-9

von Eynatten H and Tolosana Delgado R (2011). Geochemistry versus grain-size relations of sediments in the light of comminution, chemical alteration, and contrasting source rocks. In the 4th International Workshop on Compositional Data Analysis, Centre Internacional de Mètodes Numèrics en Enginyeria (CIMNE), Sant Feliu de Guíxols, Spain.

Weltje GJ and von Eynatten H (2004). Quantitative provenance analysis of sediments: Review and outlook. Sedimentary Geology, 171(1-4): 1-11. https://doi.org/10.1016/j.sedgeo.2004.05.007

Zhou X, Li A, Jiang F, and Lu J (2015). Effects of grain size distribution on mineralogical and chemical compositions: A case study from size-fractional sediments of the Huanghe (Yellow River) and Changjiang (Yangtze River). Geological Journal, 50(4): 414-433. https://doi.org/10.1002/gj.2546